



Published in final edited form as:

Cell Rep. 2015 May 5; 11(5): 727–736. doi:10.1016/j.celrep.2015.03.060.

## Increased expression of the PI3K enhancer PIKE mediates deficits in synaptic plasticity and behavior in Fragile X syndrome

Christina Gross<sup>1,9,\*</sup>, Chia-Wei Chang<sup>3</sup>, Seth M. Kelly<sup>1,7</sup>, Aditi Bhattacharya<sup>4</sup>, Sean M.J. McBride<sup>5,6</sup>, Scott W. Danielson<sup>1</sup>, Michael Q. Jiang<sup>1</sup>, Chi Bun Chan<sup>2,8</sup>, Keqiang Ye<sup>2</sup>, Jay R. Gibson<sup>3</sup>, Eric Klann<sup>4</sup>, Thomas A. Jongens<sup>5</sup>, Kenneth H. Moberg<sup>1</sup>, Kimberly M. Huber<sup>3</sup>, and Gary J. Bassell<sup>1,\*</sup>

<sup>1</sup>Department of Cell Biology, Emory University School of Medicine, Atlanta, GA 30322, USA

<sup>2</sup>Department of Pathology and Laboratory Medicine, Emory University School of Medicine, Atlanta, GA 30322, USA

<sup>3</sup>Department of Neuroscience, University of Texas Southwestern Medical Center, Dallas, Texas 75390, USA

<sup>4</sup>Center for Neural Science, New York University, New York, NY 10003, USA

<sup>5</sup>Department of Genetics, Perelman School of Medicine, University of Pennsylvania, Philadelphia, PA 19104, USA

<sup>6</sup>Department of Psychiatry, Perelman School of Medicine, University of Pennsylvania, Philadelphia, PA 19104, USA

### Summary

The PI3K enhancer PIKE links PI3K catalytic subunits to metabotropic glutamate receptors (mGlu) and activates PI3K signaling. The roles of PIKE in synaptic plasticity and the etiology of mental disorders are unknown. Here we show that increased PIKE expression is a key mediator of impaired mGlu1/5-dependent neuronal plasticity in mouse and fly models of the inherited intellectual disability Fragile X syndrome (FXS). Normalizing elevated PIKE protein levels in FXS mice reversed deficits in molecular and cellular plasticity, and improved behavior. Notably, PIKE reduction rescued PI3K-dependent and -independent neuronal defects in FXS. We further show that PI3K signaling is increased in a fly model of FXS and that genetic reduction of the

© 2015 Published by Elsevier Inc.

\*Contact: christina.gross@cchmc.org (C.G.) and gbassel@emory.edu (G.J.B.).

<sup>7</sup>Present address: Department of Biology, College of Wooster, Wooster, Ohio 44691, USA

<sup>8</sup>Present address: Department of Physiology, The University of Oklahoma Health Sciences Center, Oklahoma City, Oklahoma 73104, USA

<sup>9</sup>Present address: Division of Neurology, Cincinnati Children's Hospital Medical Center, Cincinnati, Ohio 45229, USA

**Publisher's Disclaimer:** This is a PDF file of an unedited manuscript that has been accepted for publication. As a service to our customers we are providing this early version of the manuscript. The manuscript will undergo copyediting, typesetting, and review of the resulting proof before it is published in its final citable form. Please note that during the production process errors may be discovered which could affect the content, and all legal disclaimers that apply to the journal pertain.

### Author Contributions

C.G. and G.B. conceived of the study, designed experiments and analyzed data. C.G., C.W.C., S.M.K., A.B., S.M.J.M., S.W.D., and M.Q.J. performed experiments, C.B.C and K.Y. contributed reagents, S.M.K., A.B., S.M.J.M., J.R.G., E.K., T.A.J., K.H.M., and K.M.H. analyzed and discussed data and contributed to the study design.

*Drosophila* ortholog of PIKE, CenG1A rescued excessive PI3K signaling, mushroom body defects and impaired short-term memory in these flies. Our results demonstrate a crucial role of increased PIKE expression in exaggerated mGlu1/5 signaling causing neuronal defects in FXS.

---

## Introduction

Dysregulated signaling through phosphoinositide-3 kinase (PI3K) has been recognized as a common pathological mechanism underlying diverse brain disorders, such as epilepsy, schizophrenia, intellectual disability and autism (Hoeffler and Klann, 2010; Law et al., 2012; Schick et al., 2007; Gross and Bassell 2014). Receptor-mediated PI3K/mTOR signaling plays an essential role in synaptic plasticity and neuronal function (Banko et al., 2006; Hou and Klann, 2004). Analyzing the neuronal functions of proteins that directly mediate receptor-induced activation of PI3K signaling is therefore of particular interest in order to understand molecular defects leading to mental diseases.

The PI3K enhancer PIKE (*Centg1*, a.k.a. *Agap2*) is an important regulator of receptor-mediated PI3K activity. PIKE binds and activates PI3K and Akt and plays roles in many different cellular functions, such as apoptosis, migration, and receptor trafficking (Chan and Ye, 2010). In the brain, PIKE-mediated PI3K activity downstream of group 1 metabotropic glutamate receptors (mGlu1/5) is essential for neuronal survival, leading to reduced neuronal density and decreased dendritic complexity in the neocortex of *Centg1* knockout (*Centg1*<sup>KO</sup>) mice (Chan et al., 2011b; Rong et al., 2003). PIKE's role in mGlu1/5-dependent synaptic plasticity and possible implication for the etiology of mental disorders is unknown.

The inherited intellectual disability and autism spectrum disorder Fragile X syndrome (FXS) is characterized by increased and stimulus-insensitive signaling through mGlu1/5 (Bear et al., 2004), but the underlying mechanisms are unknown. Recent phase-3 clinical trials in patients with FXS using mGlu5 negative modulators have been unsuccessful to improve the outcome measures in behavior, corroborating the critical need to better understand the mechanisms underlying dysregulated mGlu1/5 signaling in FXS. The detailed analysis of these mechanisms might reveal alternative therapeutic strategies in FXS.

FXS is caused by loss of function of the Fragile X Mental Retardation Protein (FMRP), an mRNA binding protein that binds to numerous mRNA targets and often represses their translation (Bhakar et al., 2012). Previous studies showed that *Centg1* mRNA associates with FMRP, leading to increased PIKE protein levels in *Fmr1* knockout (*Fmr1*<sup>KO</sup>) mice, a mouse model of FXS (Gross et al., 2010; Sharma et al., 2010). Whether elevated PIKE is necessary for FXS-associated phenotypes has not been studied. Due to PIKE's prominent role as a mediator of mGlu1/5-dependent PI3K activation and given the well-described, but not fully understood defect in mGlu1/5-mediated signaling and synaptic plasticity in FXS, we hypothesized that elevated PIKE expression due to loss of FMRP-mediated repression may contribute to impaired signaling, synaptic function and behavior in FXS.

To test our hypothesis that correcting PIKE expression can rescue FXS associated phenotypes, we genetically reduced PIKE in two different animal models of FXS, *Centg1* heterozygous *Fmr1*<sup>KO</sup> mice; and Centaurin Gamma-1A (*CenG1A*; the invertebrate *Centg1*

homolog) heterozygous *dFmr1* mutant *Drosophila*. Reducing PIKE, a direct target of FMRP, restored mGlu1/5-dependent molecular and cellular plasticity, and rescued behavioral and cognitive defects in both animal models. Our study uncovers a role for elevated expression of PIKE, a confirmed FMRP target, as a crucial contributor to mGlu1/5-mediated PI3K-dependent and -independent synaptic and behavioral impairments that underlie FXS.

## Results

### Genetic reduction of *Centg1* decreases PIKE protein levels and excessive PI3K activity in *Fmr1*<sup>KO</sup> mice

PIKE protein levels in the mouse brain are increased in the absence of FMRP (Gross et al., 2010; Sharma et al., 2010). To evaluate the functional impact of increased PIKE levels in FXS, we chose a strategy to genetically reduce, but not to delete, PIKE in the FXS mouse model by breeding female *Fmr1* heterozygous (*Fmr1*<sup>HET</sup>) mice with male mice heterozygous for *Centg1* (Chan et al., 2010). Male offspring of the following genotypes were analyzed: *Fmr1*<sup>WT</sup>/*Centg1*<sup>WT</sup>, *Fmr1*<sup>KO</sup>/*Centg1*<sup>WT</sup>, *Fmr1*<sup>WT</sup>/*Centg1*<sup>HET</sup>, and *Fmr1*<sup>KO</sup>/*Centg1*<sup>HET</sup> (Figure S1A). Western blot analyses validated that *Centg1* heterozygosity reduced the expression of PIKE-L protein in the cortex of *Fmr1*<sup>KO</sup> and *Fmr1*<sup>WT</sup> mice (Figure 1A).

Previous studies have shown that both PIKE-S and PIKE-L isoforms are elevated in *Fmr1*<sup>KO</sup> mice (Gross et al., 2010; Sharma et al., 2010). Due to an unspecific band at ca. 100kDa produced by the PIKE-L/S antibody available, which covered the PIKE-S-specific signals on the western blot, we were only able to quantify reduced protein levels of PIKE-L (~150kDa), the relevant isoform that links mGlu1/5 receptors to PI3K, in *Centg1* heterozygous mice (Figure 1A). To further confirm that *Centg1* heterozygous mice have reduced levels of all PIKE isoforms, we performed qRT-PCR analyses with primers detecting PIKE-A, -S and -L isoforms. All PIKE mRNA isoforms were significantly reduced in *Centg1* heterozygous mouse cortices (Figures S1B and C), suggesting that likewise all protein isoforms were reduced.

We have previously shown that activity of the PI3K catalytic subunit p110 $\beta$  is increased in the absence of FMRP (Gross and Bassell, 2012; Gross et al., 2010). Here, we show that *Centg1* heterozygosity reduced p110 $\beta$ -associated PI3K activity in *Fmr1*<sup>KO</sup> cortical synaptic fractions to wild type levels (Figure 1B).

PIKE-L links PI3K catalytic subunits to mGlu1/5 receptors via the scaffolding protein Homer (Rong et al., 2003). We thus hypothesized that elevated PIKE results in increased mGlu5-associated PI3K activity in *Fmr1*<sup>KO</sup> mice. In contrast, PI3K activity associated with PIKE-L-independent receptors, such as insulin receptor substrate 2 (IRS-2) complexes, may be unaffected. Using mGlu5-specific immunoprecipitation, we showed that mGlu5-associated PI3K activity was significantly increased in *Fmr1*<sup>KO</sup> cortex, and was reduced by *Centg1* heterozygosity in *Fmr1*<sup>KO</sup> (Figure 1C). We did not observe any significant changes in IRS-2-associated PI3K activity in *Fmr1*<sup>KO</sup> cortex, and PIKE reduction had no significant effect on IRS-2-associated PI3K activity (Figure 1D).

We have previously reported that the levels of the PI3K product phosphatidylinositol-(3,4,5)-trisphosphate (PIP3) are increased at *Fmr1*<sup>KO</sup> synapses (Gross et al., 2010). Here, we show that the ratio of PIP3 and the PI3K substrate phosphatidylinositol-(4,5)-bisphosphate (PIP2) in hippocampal acidophilic lipid fractions is increased in *Fmr1*<sup>KO</sup> mice. The increased PIP3/PIP2 ratio was normalized to wild type levels by *Centg1* heterozygosity (Figure 1E). Heterozygosity for *Centg1* had no effect on PI3K activity or PIP3/PIP2 ratios in wild type mice.

### **Genetic reduction of *Centg1* restores stimulus-induced activation of PI3K and protein synthesis in *Fmr1*<sup>KO</sup> mice**

A hallmark of FXS in the mouse model is loss of stimulus-induced signaling and protein synthesis (Gross et al., 2010; Osterweil et al., 2010; Ronesi and Huber, 2008; Sharma et al., 2010; Weiler et al., 2004), which is believed to contribute to impaired synaptic plasticity and neuronal function in FXS. To test whether reducing PIKE protein might restore this molecular plasticity in FXS, we analyzed activity-regulated PI3K function and synaptic protein synthesis in *Fmr1*<sup>KO</sup>/*Centg1*<sup>HET</sup> mice. *Centg1* heterozygosity restored mGlu1/5-mediated activation of p110 $\beta$ -associated PI3K activity after treatment with the mGlu1/5 agonist DHPG in *Fmr1*<sup>KO</sup> cortical synaptic fractions (Figure 2A), reduced excess basal protein synthesis rates (Figure 2B) and reinstated mGlu1/5-evoked stimulation of protein synthesis rates (Figure 2C). In wild type, DHPG-induced stimulation of both PI3K activity and protein synthesis was reduced by *Centg1* heterozygosity, corroborating the important function of PIKE in mediating mGlu1/5-dependent downstream signaling.

### **Genetic reduction of *Centg1* rescues excess dendritic spine density and exaggerated mGlu5-mediated LTD in *Fmr1*<sup>KO</sup> mice**

Analyses of Golgi staining in the hippocampal CA1 region of adult mice showed that *Centg1* heterozygosity reduced the elevated dendritic spine density typical for the FXS phenotype to wild type levels (Figures 2D and E, Figures S2A and B). Moreover, exaggerated mGlu1/5-dependent long term depression (LTD) in the hippocampus, a hallmark of impaired mGlu1/5-dependent synaptic plasticity in FXS, was rescued to wild type levels in *Fmr1*<sup>KO</sup> mice heterozygous for *Centg1* (Figures 2F and G).

### ***Centg1* heterozygosity reduces neocortical hyperactivity in *Fmr1*<sup>KO</sup> mice**

FXS mice display enhanced neocortical circuit activity, which can be rescued by mGlu5 negative allosteric modulators or genetic reduction of mGlu5 (Gibson et al., 2008; Goncalves et al., 2013; Hays et al., 2011). Here, we analyzed whether reduction of PIKE, which is associated with mGlu1/5 via Homer proteins, reduces neocortical activity in *Fmr1*<sup>KO</sup> mice. We measured the duration of UP states (a type of persistent activity state), which are prolonged in *Fmr1*<sup>KO</sup> thalamocortical slices, and may reflect network hyperexcitability in the absence of FMRP (Hays et al., 2011). Duration of UP states in *Fmr1*<sup>KO</sup> was significantly reduced to wild type levels by *Centg1* heterozygosity (Figures 3A and B). Prolonged UP states do not depend on protein synthesis (Hays et al., 2011), and we thus speculated that PIKE might also be mediating PI3K/mTOR-independent functions downstream of mGlu1/5. In line with this hypothesis, pre-treatment with the broad spectrum

PI3K inhibitor Wortmannin did not affect UP state duration in *Fmr1*<sup>WT</sup> or *Fmr1*<sup>KO</sup> mice (Figures S3A and B). Decreased PIKE levels also significantly reduced susceptibility to audiogenic seizures in *Fmr1*<sup>KO</sup> mice (Figure 3C).

### Genetic reduction of *Centg1* reduces repetitive behavior in *Fmr1*<sup>KO</sup> mice and improves nest building

FXS is the most common monogenic cause of autism. To test the influence of increased PIKE levels on autistic-like behaviors in the FXS mouse model, we analyzed marble burying and nest building. As reported previously, *Fmr1*<sup>KO</sup> mice buried more marbles in a given time window than their wild type littermates, which was normalized to wild type levels by *Centg1* heterozygosity (Figure 3D). Similarly, impaired nest building was improved by *Centg1* heterozygosity as measured by the amount of unused nestlet after 24 and 72 hours, and by using a nest scoring system as described previously (Deacon, 2006) (Figure 3E and F, Figures S3C–E). Interestingly, in contrast to most other phenotypes, in which *Centg1* heterozygosity did not have an effect on wild type, *Centg1* heterozygosity also improved nest building in wild type mice.

### Genetic reduction of *CenG1A*, the *Drosophila* ortholog of *Centg1*, rescues increased PI3K signaling, mushroom body defects and impaired short-term memory in *dFmr1* mutant flies

Previous studies have shown that *Drosophila* models of FXS, produced by mutations in the *Drosophila dFmr1* gene, are a valid tool to analyze molecular, cellular and behavioral deficits in FXS (McBride et al., 2013). Here we show that, similarly as in the hippocampus of *Fmr1*<sup>KO</sup> mice, PI3K signaling was elevated in flies homozygous for the strong loss-of-function allele *Fmr1*<sup>50</sup> (Zhang et al., 2001). Both PIP3/PIP2 ratios and PI3K downstream signaling, as shown by phosphorylation of S6K and Akt, were increased in *dFmr1* mutant fly heads (Figures 4A–C). To examine whether, similarly as in the mouse model, reducing the gene dosage of *CenG1A*, the fly ortholog of *Centg1* decreases PI3K signaling and reverses neuronal phenotypes observed in *dFmr1* mutant flies, we generated flies homozygous for *Fmr1*<sup>50</sup> that were heterozygous for a mutant allele of *CenG1A* (*CenG1A*<sup>EY01217</sup>). Heterozygosity of *CenG1A*<sup>EY01217</sup> significantly reduced PIP3/PIP2 ratios and PI3K downstream signaling to or below wild type levels (Figures 4A–C).

*CenG1A*<sup>EY01217</sup> also increased viability of *dFmr1* mutant flies (Figure 4D). Offspring from *Fmr1*<sup>50</sup>/TM6B X *Fmr1*<sup>50</sup>/TM6B crossings, or *CenG1A*<sup>EY01217</sup>/CyO;*Fmr1*<sup>50</sup>/TM6B X *Fmr1*<sup>50</sup>/TM6B, respectively, were genotyped and counted at P0 or P1 following eclosion. The values shown are percentages of flies homozygous for the *dFmr1* null gene generated by these crossings.

*dFmr1* mutant mushroom bodies, which are bilaterally symmetric axonal projections from Kenyon neurons, show a high rate of  $\beta$ -lobe fusion across the midline (Michel et al., 2004). Heterozygosity for the *CenG1A*<sup>EY01217</sup> allele rescued this developmental defect in the *dFmr1* mutant background, but did not affect gross mushroom body morphology in wild type (Figure 4E).

We next tested whether *CenG1A* heterozygosity improved the impairment in short-term memory in *dFmr1* mutant flies. When exposed to an unreceptive (previously mated) female,

male wild type flies learn to reduce mating behavior, and retain this memory over 2–3 hours. As shown previously (McBride et al., 2005), *dFmr1* mutant flies had impaired short-term memory of courtship suppression, and *CenG1A*<sup>EY01217</sup> heterozygosity rescued this cognitive defect (Figure 4F, Figure S4B). Notably, *CenG1A*<sup>EY01217</sup> heterozygous flies had impaired short-term memory as well, suggesting that this type of memory in flies is dosage-sensitive to PIKE.

## Discussion

The goal of this study was to test the hypothesis that increased expression of the PI3K enhancer PIKE, which is translationally regulated by FMRP and an important regulator of mGlu1/5-dependent PI3K activity, contributes to dysregulated mGlu1/5-dependent synaptic plasticity and neuronal function underlying the pathogenesis of FXS. To this end, we used genetic approaches in a mouse and a fly model to reduce PIKE levels in FXS. Previous studies have genetically reduced or deleted components upstream and downstream of the PI3K signaling complex, but these were not direct mRNA targets of FMRP, nor were they shown to be translated in excess in FXS (Bathacharya et al., 2012; Dolen et al., 2007, Ronesi et al., 2012). Moreover, in most cases, the approach taken thus far has been to delete a gene of interest, hence an advantage of the genetic reduction approach taken here is to compensate for loss of translational repression of FMRP-associated mRNAs in FXS. Here we show that this strategy rescued FXS-associated phenotypes on several functional levels, from signaling mechanisms to synaptic plasticity and memory, including PI3K- and protein synthesis-dependent and -independent neuronal functions. We further corroborate the importance of PIKE dysregulation for the etiology of FXS by showing that PI3K signaling is increased in a fly model of FXS, and that reducing the *Drosophila* ortholog of PIKE, *CenG1A* in FXS flies rescues molecular, morphological and cognitive defects. Taken together, our study suggests that gain of function of a critical molecular linker of the mGlu5-PI3K signaling complex contributes to FXS-associated defects in neuronal and behavioral function.

### Receptor-specific PI3K signaling defects in FXS

Numerous studies have reported exaggerated signaling of mGlu1/5 receptors in FXS animal models (Dolen et al., 2007; Huber et al., 2002; Muddashetty et al., 2007; Osterweil et al., 2010; Ronesi et al., 2012), and mGlu5 negative allosteric modulators have been shown to rescue many FXS-associated phenotypes (McBride et al., 2005; Michalon et al., 2012; Yan et al., 2005). Several recent studies have begun to analyze the molecular mechanisms of dysregulated mGlu1/5 signaling in FXS by genetically reducing or deleting mGlu1/5 signaling complex components or downstream regulators of protein synthesis (Bhattacharya et al., 2012; Dolen et al., 2007; Ronesi et al., 2012), but the detailed underlying molecular mechanisms are still unknown. In this study, we show that the PI3K enzymatic activity of the mGlu5 protein complex is increased in *Fmr1*<sup>KO</sup> cortex, and rescued by *Centg1* heterozygosity (Figure 1C), which provides direct evidence for a link between impaired mGlu1/5 signaling, excessive PI3K activity and loss of translational control of FMRP target mRNAs in FXS. In contrast, IRS-2-associated PI3K activity is not significantly altered in *Fmr1*<sup>KO</sup> mice (Figure 1D). This supports a direct role of the mGlu1/5-PI3K signaling

complex in mediating neuronal defects in FXS (Ronesi et al., 2012) and gives rise to the hypothesis that FMRP is not a regulator of general PI3K signaling, but controls a specific subset or network of the PI3K signaling complex in neurons via regulation of proteins that tether PI3K activity to certain receptors (Figure 5).

### **Reducing PIKE rescues impairments in stimulus-induced signaling and protein synthesis, dendritic spine morphology and synaptic plasticity in *Fmr1*<sup>KO</sup> mice**

The capability of a neuron to adjust intracellular signaling and synthesize new proteins in response to external stimuli is essential for enduring forms of synaptic plasticity underlying behavior and cognition (Sutton and Schuman, 2006). In FMRP-deficient neurons, basal activity of the PI3K subunit p110 $\beta$  and general protein synthesis are increased and stimulus-insensitive (Gross et al., 2010; Osterweil et al., 2010; Weiler et al., 2004). Here, we show that genetic reduction of *Centg1* restored mGlu1/5-induced increases in protein synthesis and p110 $\beta$  activity in *Fmr1*<sup>KO</sup> mice (Figures 2A–C). Our observations suggest that PIKE is a key mediator of FMRP's function to control activity-mediated neuronal signaling and protein synthesis and thus synaptic plasticity. Further corroborating these results, *Centg1* heterozygosity rescued exaggerated mGluR-LTD in *Fmr1*<sup>KO</sup> hippocampus (Figures 2F and G), and reduced the increased dendritic spine density in hippocampal CA1 neurons from *Fmr1*<sup>KO</sup> mice (Figures 2D and E).

We noticed that for most of the tested molecular, cellular or behavioral phenotypes, *Centg1* heterozygosity had no significant effects in wild type mice, although PIKE protein levels were reduced. We speculate that in wild type, reduced levels of PIKE are compensated by other known modes of PI3K activation, for example heterotrimeric G proteins (Guillermet-Guibert et al., 2008). However, neurons seem vulnerable to elevated and unregulated PIKE in the absence of FMRP, suggesting that increased PIKE plays an important and specific role in FXS-associated phenotypes.

### **A role for increased expression of PIKE in PI3K-independent neocortical hyperactivity and in impaired behavior in *Fmr1*<sup>KO</sup> mice**

Loss of FMRP in patients and animal models leads to increased susceptibility to epileptic seizures, increased neuronal network activity and general neuronal hyperexcitability (Goncalves et al., 2013; Hays et al., 2011). Here, we show that genetic reduction of PIKE reduces the prolonged duration of bursts of spontaneous neocortical activity (UP states; Figures 3A and B) that are observed in *Fmr1*<sup>KO</sup> mice (Hays et al., 2011). Notably, while UP states are sensitive to mGlu5 inhibition, they do not depend on new protein synthesis (Hays et al., 2011) or on PI3K signaling (Figures S3A and B), suggesting additional roles of PIKE in mGlu1/5 function apart from PI3K/mTOR-mediated protein synthesis, for example, through PIKE-L association with Homer and regulation of Homer scaffolds, which are dysregulated in FXS (Ronesi et al., 2012). Moreover, PIKE isoforms were shown to have other roles apart from PI3K activation, which could also contribute to the observed rescue of UP states, such as direct binding of PIKE-L to GluA2 and GRIP2 (Chan et al., 2011a).

*Centg1* heterozygosity also significantly reduces the susceptibility to audiogenic seizures in *Fmr1*<sup>KO</sup> mice (Figure 3C). Absence of PIKE in *Centg1*<sup>KO</sup> mice leads to higher

susceptibility to kainic acid-induced excitotoxicity and seizures (Chan et al., 2012). Our results suggest that *Centg1* heterozygosity reduces neuronal excitability also in wild type, although none of the effects were significant. Reduced PIKE levels may thus protect neurons from hyperactivity in these experimental settings.

Genetic reduction of *Centg1* rescued impaired nesting behavior and obsessive marble burying in *Fmr1*<sup>KO</sup> mice (Figures 3D–F), suggesting a role of increased PIKE in autistic-like behavior. Increased PI3K/mTOR signaling has been implicated in autism, but the *Centg1* gene has not been previously associated with autism susceptibility.

### Improvement of neuronal function by genetic reduction of PIKE in FXS is conserved across species

Here, we show that increased PI3K signaling occurs in a *Drosophila* model of FXS and can also be genetically targeted to correct phenotypes. Genetic reduction of the *Drosophila Centg1* ortholog *CenG1A* reduces excess PI3K signaling, and rescues lethality, axonal overgrowth, as well as impaired short-term memory caused by the absence of dFMR1 (Figure 4). These findings in the fly model are similar to observations in *Fmr1*<sup>KO</sup> mice, and thus suggest a conserved function of FMRP to regulate PIKE and PI3K signaling. However, as of now, it is not known if *CenG1A* mRNA is a target of dFMR1 in flies, and more work is needed to identify dFMR1 mRNA targets in flies that are translationally dysregulated in *dFmr1* mutant flies.

While PIP3/PIP2 ratios in *CenG1A* heterozygous flies were reduced in both wild type and *dFmr1* mutant background, downstream signaling and gross mushroom body morphology were not affected in wild type. However, *CenG1A* heterozygous flies were impaired in courtship memory, suggesting a PIKE dosage-sensitive regulation of this type of cognition. Given these results and the importance of PI3K signaling in axonal growth and guidance in the *Drosophila* visual system (Song et al., 2003), we speculate that *CenG1A* heterozygosity could have caused some more subtle defects in mushroom body morphology in wild type flies that were not detected by our assessment of FXS-typical fusion of  $\beta$ -lobes. Our results showing a dosage-sensitivity of memory function to PIKE and PI3K activity are in line with earlier reports showing that learning in flies is dosage-sensitive to the cAMP-signaling pathway: both the *dunce* mutant, which is impaired in cAMP phosphodiesterase, as well as the *rutabaga* mutant, which has a gene defect in Ca<sup>2+</sup>/calmodulin-dependent adenylate cyclase, are impaired in associative learning (Tully and Quinn, 1985). These observations suggest that, similarly as in the case of PIKE and PI3K activity, either too much or too little cAMP signaling can have adverse effects on cognitive function.

Our study reveals that genetically reducing PIKE, a confirmed FMRP target, can rescue diverse FXS-associated phenotypes at the molecular, physiological and behavioral levels in animal models. These findings provide insight into the mechanisms of dysregulated mGlu1/5-signaling in the absence of FMRP by showing that reducing the increased expression of PIKE, a critical mediator of mGlu1/5-dependent downstream signaling, rescues FXS-associated neuronal impairments on multiple levels. Notably, this strategy rescues protein synthesis-dependent (LTD) and -independent neuronal defects (UP states) in FXS, suggesting that increased PIKE is not just a mediator of dysregulated protein synthesis,



but plays additional roles in mTOR- and protein synthesis-independent dysfunctions of the mGlu1/5 complex in the absence of FMRP (Figure 5). So far, it is unknown if the observed rescue is mediated mainly by reduction of the long isoform of PIKE that tethers mGlu1/5 to downstream PI3K signaling, or if the overall reduction of all PIKE isoforms underlies the improvement of FXS-associated phenotypes. In the future, to further test the mGluR theory of FXS, it will be interesting to explore if targeting specifically the long isoform of PIKE e.g. through blocking interactions of PIKE with mGlu1/5 receptor complexes may also rescue phenotypes in the FXS mouse model.

## Experimental Procedures

### Mice and Flies

Mice were generated by crossing female *Fmr1*<sup>HET</sup> mice (*The Jackson Laboratory*) with male *Centg1* heterozygous mice (Chan et al., 2010), and were genotyped by PCR. The animal protocol was approved by the Institutional Animal Care and Use Committees of Emory University, UT Southwestern, NYU and CCHMC, and complied with the Guide for the Care and Use of Laboratory Animals. Flies were maintained at 25°C under standard conditions. Wild type *Oregon-R*, wild type *w1118* (for behavioral analyses), *dFmr1* (*dFmr1*<sup>50M/TM6B</sup>) (Zhang et al., 2001) and *CenG1A* (*CenG1A*<sup>EY01217/CyO</sup>) alleles were obtained from the Bloomington Drosophila Stock Center. For details, see Supplemental Experimental Procedures.

### Antibodies

The following antibodies were used: rabbit polyclonal anti-FMRP (*Sigma*, F4055), mouse monoclonal anti- $\alpha$ Tubulin (clone DM1A, *Sigma*), rabbit polyclonal anti-p110 $\beta$  (*Millipore*, 09–482), rabbit polyclonal anti-PIKE-L/S (*Millipore*, 07–675), rabbit polyclonal anti-mGlu5 (*Millipore*, AB5675), mouse monoclonal anti-dFMR1 (clone 6A15, *Abcam*), and mouse monoclonal anti-fasciclin II (clone 1D4, *NeuroMab*). The following rabbit monoclonal antibodies from *Cell Signaling Technology* were used: phospho-Akt(Thr308) (#4056), phospho-Drosophila p70 S6 Kinase (Thr398) (#9209), IRS-2 (#4502).

### Drugs and Reagents

(*S*)-3,5-Dihydroxyphenylglycine (DHPG) was obtained from *Tocris Bioscience*, and dissolved in water or ACSF for LTD experiments. 50 mM stock solutions were kept in aliquots at –80°C, except for LTD experiments (prepared freshly on the day of the experiment). Wortmannin (*Tocris Bioscience*) was dissolved in DMSO (10  $\mu$ M) and kept in aliquots at –80°C. For metabolic labeling, EXPRE<sup>35</sup>S<sup>35</sup>S Protein Labeling Mix (*Perkin Elmer*) was used.

### Immunoprecipitation (IP) and Western Blotting

IRS-2- and mGlu5-specific protein complexes were immunoprecipitated from cortical lysates, and p110 $\beta$ -complexes were immunoprecipitated from synaptoneurosome preparations (Gross et al., 2010) for PI3K activity ELISAs, using IRS-2-, mGlu5-, or p110 $\beta$ -selective antibodies. Briefly, for mGlu5-, IRS-2- and p110 $\beta$ -IPs, fresh or snap-frozen cortices, or freshly prepared synaptic fractions, respectively, were homogenized in PI3K

assay lysis buffer as described previously (Gross et al., 2010) and equal amounts of protein were incubated with antibody or IgG 5 hours or overnight rotating at 4°C. Antibody-complexes were pulled down using protein A-agarose, washed in lysis buffer and subjected to PI3K assays. For western blotting, proteins were resolved on SDS-polyacrylamide gels, transferred to PVDF-membranes and detected using horseradish peroxidase-coupled secondary antibodies and enhanced chemiluminescence.

### **PI3K Assays and PIP2/PIP3 Mass ELISAs**

PI3K activity was measured using PI3-Kinase Activity ELISA: Pico (*Echelon Biosciences, Inc.*), and PIP2 and PIP3 contents of acidophilic lipids were quantified using PI(3,4,5)P<sub>3</sub> and PI(4,5)P<sub>2</sub> mass ELISA kits (*Echelon Biosciences, Inc.*) following the manufacturer's protocol. For details, see Supplemental Experimental Procedures.

### **Metabolic Labeling**

Protein synthesis rates were quantified in synaptoneurosome using 35-S-methionine metabolic labeling under basal conditions or following mGlu1/5-stimulation (20 min DHPG, 100 μM at 37°C) as described in Gross et al., 2010. For details, see Supplemental Experimental Procedures.

### **Dendritic Spine Analysis**

Brains from mice at postnatal days 58–62 were Golgi-stained using the FD Rapid GolgiStain™ Kit (*FD NeuroTechnologies, Inc*) according to the manufacturer's protocol. Briefly, brains were dissected on ice and then immersed for 14–18 days in impregnation solution, with one solution change within the first 24 hours. Brains were cut in 160 μm slices using a *Leica* vibratome, mounted on coverslips and stained according to the manufacturer's protocol. Secondary, apical dendrites from pyramidal CA1 neurons were imaged using a 60x oil DIC objective for a minimum length of 60 μm starting from their origin at the primary dendritic shaft. In most cases, z-stacks were taken to ensure tracing of the dendrite throughout the entire length. Dendritic spines were counted and recorded as a function of 10 μm segments on the dendrites using Fiji Imaging software. Dendrites were between 60 and 120 μm in length. We analyzed three to five brains per genotype, four to eight neurons per brain, and one dendrite per neuron.

### **Audiogenic Seizures**

Mice were tested in a plastic chamber covered with a Styrofoam lid containing a 120-dB personal security alarm as described in Ronesi et al., 2012. The alarm was presented to the mice for 5 min. Mice were observed or video-taped during the entire procedure, full tonic-clonic seizure (sometimes followed by death caused by respiratory arrest) was counted as positive, wild running behavior was not counted as seizure.

### **UP States**

UP states were performed as described previously (Hays et al., 2011). For details see Supplemental Experimental Procedures.

### Hippocampal mGluR-LTD

DHPG-induced mGluR-LTD on brain slices was performed as described previously (Bhattacharya et al., 2012). For details see Supplemental Experimental Procedures.

### Nest Building Behavior

Nest building was assessed as described in Deacon, 2006. Briefly, male mice at postnatal day 30 were placed in a fresh cage with standard bedding supplemented with 3g of fresh nestlet between 4 and 6pm at the start of the experiment. 72 hours later, nests were assessed using the score proposed by Deacon 2006, unused nestlet was weighed, and all nestlet material was replaced by 3g of fresh nestlet. After 24 hours, nests were assessed as described above.

### Marble Burying

Marble burying was assessed as described previously (Bhattacharya et al., 2012), with the following modifications. Twenty dark blue small glass beads were placed in a 5 × 4 grid on fresh 8 cm deep bedding. Mice were left in the cage for 15 min. Marbles covered 50% or more were scored as “buried”. Mice were always tested between 12 and 3 pm. Mice were tested in nesting behavior prior to the marble burying assay.

### Analysis of *Drosophila* Mushroom Body Morphology

Flies were collected at days 0 to 2 post-eclosion. For western blot analyses and PIP3/PIP2 quantifications fly heads were dissected on dry ice and stored at –80°C until further processing. For mushroom body analyses fly brains were dissected and immediately fixed in 4% PFA, processed for anti-Fasciclin II staining (Wu and Luo, 2006) and mounted on microscope slides using VectaMount AQ aqueous mounting medium (*Vector Laboratories*). Sections were imaged using a Zeiss LSM 710 confocal, or a Leica SP8 Multi Photon microscope and processed using ImageJ (*NIH*). Brains were analyzed for β-lobe fusion across the midline as described previously (Michel et al., 2004).

### Analysis of *Drosophila* Courtship Behavior

Courtship short term memory was assessed as described previously (McBride et al., 2005). Briefly, virgin male flies were collected within 4 hours of eclosion, aged for 5–7 days and transferred to fresh food in individual small food tubes the night before testing. Virgin females were collected within 2 hours of eclosion and kept in groups of 10–15. Mated females were observed to mate with a male the night before training. The courtship index (CI) was calculated as the percentage of time spent courting during the observation time, which was either 10 min or until successful copulation (Siegel and Hall, 1979). Memory index was calculated as the relative difference between the mean courtship index (CI) of trained and naïve flies  $((CI(\text{naïve}) - CI(\text{trained})) / CI(\text{naïve}))$  (Keleman et al., 2012).

### Western Blot Quantification

For western blot analyses, equal amounts of protein were loaded, and western blots were quantified densitometrically using ImageJ (*NIH*), and normalized to α-tubulin.

## Data Acquisition and Statistical Analyses

Experimenters were blind to the genotype at the time of the experiments. All statistics were performed with SigmaStat v.3.1, GraphPad Prism6 or SPSS, using the appropriate tests as indicated in each figure. For details, see Supplemental Experimental Procedures.

## Supplementary Material

Refer to Web version on PubMed Central for supplementary material.

## Acknowledgements

This research was supported by the FRAXA Research Foundation (C.G., S.M.J.M., T.A.J.), Brain and Behavior Research Foundation NARSAD Distinguished Investigator Grant (G.J.B.), Autism Speaks Pilot Grant (C.G.), Charles H. Revson Foundation Senior Biomedical Fellowship (A.B.), University of Pennsylvania R25 MH060490 (Clinical Research Scholars Program in Psychiatry) (S.M.J.M.), NIH grants MH105353 (G.J.B. and C.G.), NS045711 (K.M.H.), HD056370 (J.R.G.), NS034007 and NS047384 (E.K.), DOD-Autism (AR1101189) (T.A.J.), Emory University Center for Translational Social Neuroscience Pilot Grant (G.B.), Emory University Children's Center for Neuroscience Pilot Grant (G.B., C.G.), and the Integrated Cellular Imaging Microscopy and Viral Vector Cores of the Emory Neuroscience NINDS Core Facilities grant, P30NS055077. The authors thank Ashwini Poopal and Lindsay Schroeder for technical assistance. We thank Dr. Sharon Swanger for critically reading an earlier version of the manuscript, as well as members of the G.J.B., K.H.M. and K.M.H. labs for discussions.

## References

- Banko JL, Hou L, Poulin F, Sonenberg N, Klann E. Regulation of eukaryotic initiation factor 4E by converging signaling pathways during metabotropic glutamate receptor-dependent long-term depression. *J Neurosci*. 2006; 26:2167–2173. [PubMed: 16495443]
- Bear MF, Huber KM, Warren ST. The mGluR theory of fragile X mental retardation. *Trends Neurosci*. 2004; 27:370–377. [PubMed: 15219735]
- Bhakar AL, Dolen G, Bear MF. The pathophysiology of fragile X (and what it teaches us about synapses). *Annual review of neuroscience*. 2012; 35:417–443.
- Bhattacharya A, Kaphzan H, Alvarez-Dieppa AC, Murphy JP, Pierre P, Klann E. Genetic removal of p70 S6 kinase 1 corrects molecular, synaptic, and behavioral phenotypes in fragile X syndrome mice. *Neuron*. 2012; 76:325–337. [PubMed: 23083736]
- Chan CB, Chen Y, Liu X, Papale L, Escayg A, Mei L, Ye K. Essential role of PIKE GTPases in neuronal protection against excitotoxic insults. *Advances in biological regulation*. 2012; 52:66–76. [PubMed: 21925531]
- Chan CB, Chen Y, Liu X, Tang X, Lee CW, Mei L, Ye K. PIKE-mediated PI3-kinase activity is required for AMPA receptor surface expression. *EMBO J*. 2011a; 30:4274–4286. [PubMed: 21847098]
- Chan CB, Liu X, Pradoldej S, Hao C, An J, Yepes M, Luo HR, Ye K. Phosphoinositide 3-kinase enhancer regulates neuronal dendritogenesis and survival in neocortex. *J Neurosci*. 2011b; 31:8083–8092. [PubMed: 21632930]
- Chan CB, Liu X, Ensslin MA, Dillehay DL, Ormandy CJ, Sohn P, Serra R, Ye K. PIKE-A is required for prolactin-mediated STAT5a activation in mammary gland development. *EMBO J*. 2010; 29:956–968. [PubMed: 20075866]
- Chan CB, Ye K. Multiple functions of phosphoinositide-3 kinase enhancer (PIKE). *Scientific World Journal*. 2010; 10:613–623. [PubMed: 20419274]
- Darnell JC, Van Driesche SJ, Zhang C, Hung KY, Mele A, Fraser CE, Stone EF, Chen C, Fak JJ, Chi SW, et al. FMRP stalls ribosomal translocation on mRNAs linked to synaptic function and autism. *Cell*. 2011; 146:247–261. [PubMed: 21784246]
- Deacon RM. Assessing nest building in mice. *Nat Protoc*. 2006; 1:1117–1119. [PubMed: 17406392]
- Dolen G, Osterweil E, Rao BS, Smith GB, Auerbach BD, Chattarji S, Bear MF. Correction of fragile X syndrome in mice. *Neuron*. 2007; 56:955–962. [PubMed: 18093519]

- Gibson JR, Bartley AF, Hays SA, Huber KM. Imbalance of neocortical excitation and inhibition and altered UP states reflect network hyperexcitability in the mouse model of fragile X syndrome. *J Neurophysiol.* 2008; 100:2615–2626. [PubMed: 18784272]
- Goncalves JT, Anstey JE, Golshani P, Portera-Cailliau C. Circuit level defects in the developing neocortex of Fragile X mice. *Nat Neurosci.* 2013; 16:903–909. [PubMed: 23727819]
- Gross C, Bassell GJ. Excess Protein Synthesis in FXS Patient Lymphoblastoid Cells Can Be Rescued with a p110beta-Selective Inhibitor. *Mol Med.* 2012; 18:336–345. [PubMed: 22207187]
- Gross C, Bassell GJ. Neuron-specific regulation of class I PI3K catalytic subunits and their dysfunction in brain disorders. *Frontiers in molecular neuroscience.* 2014; 7:12. [PubMed: 24592210]
- Gross C, Nakamoto M, Yao X, Chan CB, Yim SY, Ye K, Warren ST, Bassell GJ. Excess phosphoinositide 3-kinase subunit synthesis and activity as a novel therapeutic target in fragile X syndrome. *J Neurosci.* 2010; 30:10624–10638. [PubMed: 20702695]
- Guillermet-Guibert J, Bjorklof K, Salpekar A, Gonella C, Ramadani F, Bilancio A, Meek S, Smith AJ, Okkenhaug K, Vanhaesebroeck B. The p110beta isoform of phosphoinositide 3-kinase signals downstream of G protein-coupled receptors and is functionally redundant with p110gamma. *Proc Natl Acad Sci U S A.* 2008; 105:8292–8297. [PubMed: 18544649]
- Hays SA, Huber KM, Gibson JR. Altered neocortical rhythmic activity states in Fmr1 KO mice are due to enhanced mGluR5 signaling and involve changes in excitatory circuitry. *J Neurosci.* 2011; 31:14223–14234. [PubMed: 21976507]
- Hoeffler CA, Klann E. mTOR signaling: at the crossroads of plasticity, memory and disease. *Trends Neurosci.* 2010; 33:67–75. [PubMed: 19963289]
- Hou L, Klann E. Activation of the phosphoinositide 3-kinase-Akt-mammalian target of rapamycin signaling pathway is required for metabotropic glutamate receptor-dependent long-term depression. *J Neurosci.* 2004; 24:6352–6361. [PubMed: 15254091]
- Huber KM, Gallagher SM, Warren ST, Bear MF. Altered synaptic plasticity in a mouse model of fragile X mental retardation. *Proc Natl Acad Sci U S A.* 2002; 99:7746–7750. [PubMed: 12032354]
- Keleman K, Vrontou E, Kruttner S, Yu JY, Kurtovic-Kozaric A, Dickson BJ. Dopamine neurons modulate pheromone responses in *Drosophila* courtship learning. *Nature.* 2012; 489:145–149. [PubMed: 22902500]
- Law AJ, Wang Y, Sei Y, O'Donnell P, Piantadosi P, Papaleo F, Straub RE, Huang W, Thomas CJ, Vakkalanka R, et al. Neuregulin 1-ErbB4-PI3K signaling in schizophrenia and phosphoinositide 3-kinase-p110delta inhibition as a potential therapeutic strategy. *Proc Natl Acad Sci U S A.* 2012; 109:12165–12170. [PubMed: 22689948]
- McBride SM, Choi CH, Wang Y, Liebelt D, Braunstein E, Ferreira D, Sehgal A, Siwicki KK, Dockendorff TC, Nguyen HT, et al. Pharmacological rescue of synaptic plasticity, courtship behavior, and mushroom body defects in a *Drosophila* model of fragile X syndrome. *Neuron.* 2005; 45:753–764. [PubMed: 15748850]
- McBride SMJ, Holloway SL, Jongens TA. Using *Drosophila* as a tool to identify pharmacological therapies for fragile X syndrome. *Drug Discovery Today: Technologies.* 2013; 10:e129–e136. [PubMed: 24050241]
- Michalon A, Sidorov M, Ballard TM, Ozmen L, Spooren W, Wettstein JG, Jaeschke G, Bear MF, Lindemann L. Chronic pharmacological mGlu5 inhibition corrects fragile X in adult mice. *Neuron.* 2012; 74:49–56. [PubMed: 22500629]
- Michel CI, Kraft R, Restifo LL. Defective neuronal development in the mushroom bodies of *Drosophila* fragile X mental retardation 1 mutants. *J Neurosci.* 2004; 24:5798–5809. [PubMed: 15215302]
- Muddashetty RS, Kelic S, Gross C, Xu M, Bassell GJ. Dysregulated metabotropic glutamate receptor-dependent translation of AMPA receptor and postsynaptic density-95 mRNAs at synapses in a mouse model of fragile X syndrome. *J Neurosci.* 2007; 27:5338–5348. [PubMed: 17507556]
- Osterweil EK, Krueger DD, Reinhold K, Bear MF. Hypersensitivity to mGluR5 and ERK1/2 leads to excessive protein synthesis in the hippocampus of a mouse model of fragile X syndrome. *J Neurosci.* 2010; 30:15616–15627. [PubMed: 21084617]

- Ronesi JA, Huber KM. Homer interactions are necessary for metabotropic glutamate receptor-induced long-term depression and translational activation. *J Neurosci*. 2008; 28:543–547. [PubMed: 18184796]
- Ronesi JA, Collins KA, Hays SA, Tsai NP, Guo W, Birnbaum SG, Hu JH, Worley PF, Gibson JR, Huber KM. Disrupted Homer scaffolds mediate abnormal mGluR5 function in a mouse model of fragile X syndrome. *Nat Neurosci*. 2012; 15:431–440. S431. [PubMed: 22267161]
- Rong R, Ahn JY, Huang H, Nagata E, Kalman D, Kapp JA, Tu J, Worley PF, Snyder SH, Ye K. PI3 kinase enhancer-Homer complex couples mGluRI to PI3 kinase, preventing neuronal apoptosis. *Nat Neurosci*. 2003; 6:1153–1161. [PubMed: 14528310]
- Schick V, Majores M, Koch A, Elger CE, Schramm J, Urbach H, Becker AJ. Alterations of phosphatidylinositol 3-kinase pathway components in epilepsy-associated glioneuronal lesions. *Epilepsia* 48 Suppl. 2007; 5:65–73.
- Sharma A, Hoeffler CA, Takayasu Y, Miyawaki T, McBride SM, Klann E, Zukin RS. Dysregulation of mTOR Signaling in Fragile X Syndrome. *J Neurosci*. 2010; 30:694–702. [PubMed: 20071534]
- Siegel RW, Hall JC. Conditioned responses in courtship behavior of normal and mutant *Drosophila*. *Proc Natl Acad Sci U S A*. 1979; 76:3430–3434. [PubMed: 16592682]
- Song J, Wu L, Chen Z, Kohanski RA, Pick L. Axons guided by insulin receptor in *Drosophila* visual system. *Science*. 2003; 300:502–505. [PubMed: 12702880]
- Sutton MA, Schuman EM. Dendritic protein synthesis, synaptic plasticity, and memory. *Cell*. 2006; 127:49–58. [PubMed: 17018276]
- Tully T, Quinn WG. Classical conditioning and retention in normal and mutant *Drosophila melanogaster*. *Journal of comparative physiology A, Sensory, neural, and behavioral physiology*. 1985; 157:263–277.
- Weiler IJ, Spangler CC, Klintsova AY, Grossman AW, Kim SH, Bertaina-Anglade V, Khaliq H, de Vries FE, Lambers FA, Hatia F, et al. Fragile X mental retardation protein is necessary for neurotransmitter-activated protein translation at synapses. *Proc Natl Acad Sci U S A*. 2004; 101:17504–17509. [PubMed: 15548614]
- Wu JS, Luo L. A protocol for dissecting *Drosophila melanogaster* brains for live imaging or immunostaining. *Nat Protoc*. 2006; 1:2110–2115. [PubMed: 17487202]
- Yan QJ, Rammal M, Tranfaglia M, Bauchwitz RP. Suppression of two major Fragile X Syndrome mouse model phenotypes by the mGluR5 antagonist MPEP. *Neuropharmacology*. 2005; 49:1053–1066. [PubMed: 16054174]
- Zhang YQ, Bailey AM, Matthies HJ, Renden RB, Smith MA, Speese SD, Rubin GM, Broadie K. *Drosophila* fragile X-related gene regulates the MAP1B homolog Futsch to control synaptic structure and function. *Cell*. 2001; 107:591–603. [PubMed: 11733059]

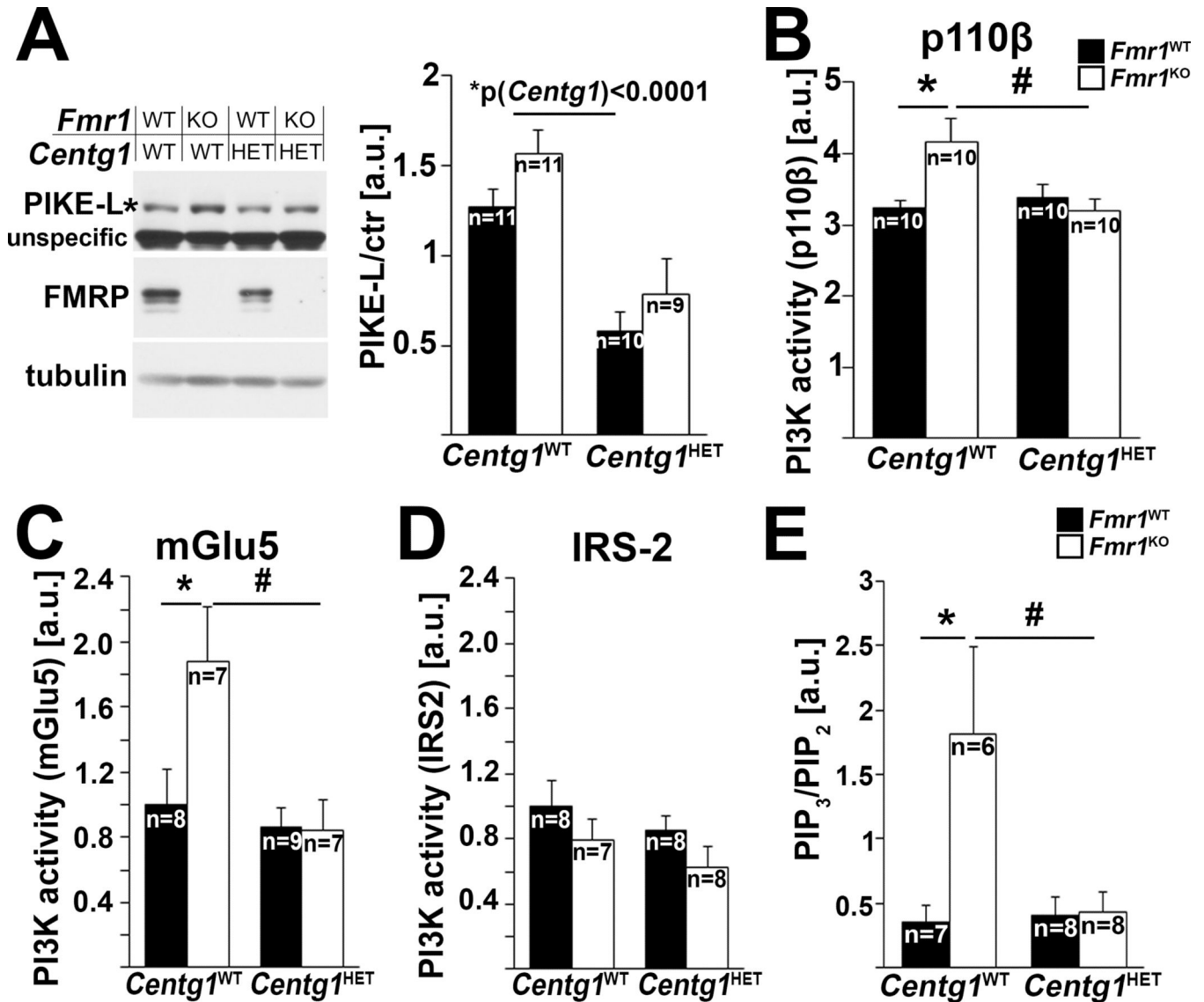


**Figure 1. Genetic reduction of PIKE expression decreases elevated PI3K activity in the cortex of *Fmr1*<sup>KO</sup> mice**

(A) *Centg1* heterozygosity reduces PIKE-L protein levels in both *Fmr1*<sup>WT</sup> and *Fmr1*<sup>KO</sup> background (2-way ANOVA, significant effect of *Centg1* heterozygosity on PIKE-L protein levels ( $F(1,37)=29.94$ ,  $p<0.0001$ ), no effect of *Fmr1*<sup>KO</sup> ( $F(1,37)=3.462$ ,  $p=0.0708$ ), no interaction ( $F(1,37)=0.1241$ ,  $p=0.7266$ )). Representative western blots are shown at the left. Protein levels were normalized to  $\alpha$ -tubulin. Also see Figure S1A for breeding scheme and Figures S1B and C for quantification of PIKE mRNA levels in *Centg1* heterozygous mice. (B–D) Increased p110 $\beta$ - and mGlu5-associated PI3K activity is reduced to WT levels in cortical synaptic fractions (p110 $\beta$ ) or cortical lysates (mGlu5) from *Centg1* heterozygous *Fmr1*<sup>KO</sup> mice, whereas IRS2-associated PI3K activity is not affected by *Fmr1* or *Centg1* genotype. PI3K enzymatic activity of p110 $\beta$ -, mGlu5- or IRS-2-specific immunoprecipitates was measured by ELISA (B, 2-way ANOVA,  $p(Fmr1)=0.079$ ,  $F(1,36)=3.275$ ;  $p(Centg1)=0.053$ ,  $F(1,36)=4.013$ ;  $p(interaction)=0.011$ ,  $F(1,36)=7.255$ ; \* $p=0.015$ ,

#p=0.011; **C**, 2-way ANOVA,  $p(Fmr1)=0.08$ ,  $F(1, 27)=3.320$ ;  $p(Centg1)=0.018$ ,  $F(1,27)=6.35$ ;  $p(interaction)=0.036$ ,  $F(1,27)=4.892$ ; \*p=0.042, #p=0.017; **D**, 2-way ANOVA,  $p(Fmr1)=0.115$ ,  $F(1, 27)=2.659$ ,  $p(Centg1)=0.228$ ,  $F(1,27)=1.52$ ;  $p(interaction)=0.947$ ,  $F(1,27)=0.005$ .

**(E)** Elevated PIP3/PIP2 ratios in *Fmr1*<sup>KO</sup> hippocampus are significantly decreased by genetic reduction of *Centg1* (2-way ANOVA,  $p(Fmr1)=0.0225$ ,  $F(1, 25)=5.919$ ;  $p(Centg1)=0.0398$ ,  $F(1,25)=4.702$ ;  $p(interaction)=0.0275$ ,  $F(1,25)=5.478$ ; \*p=0.0179, #p=0.0218).

Error bars represent SEM, n represents individual mice from at least 5 litters, n indicated in each figure.



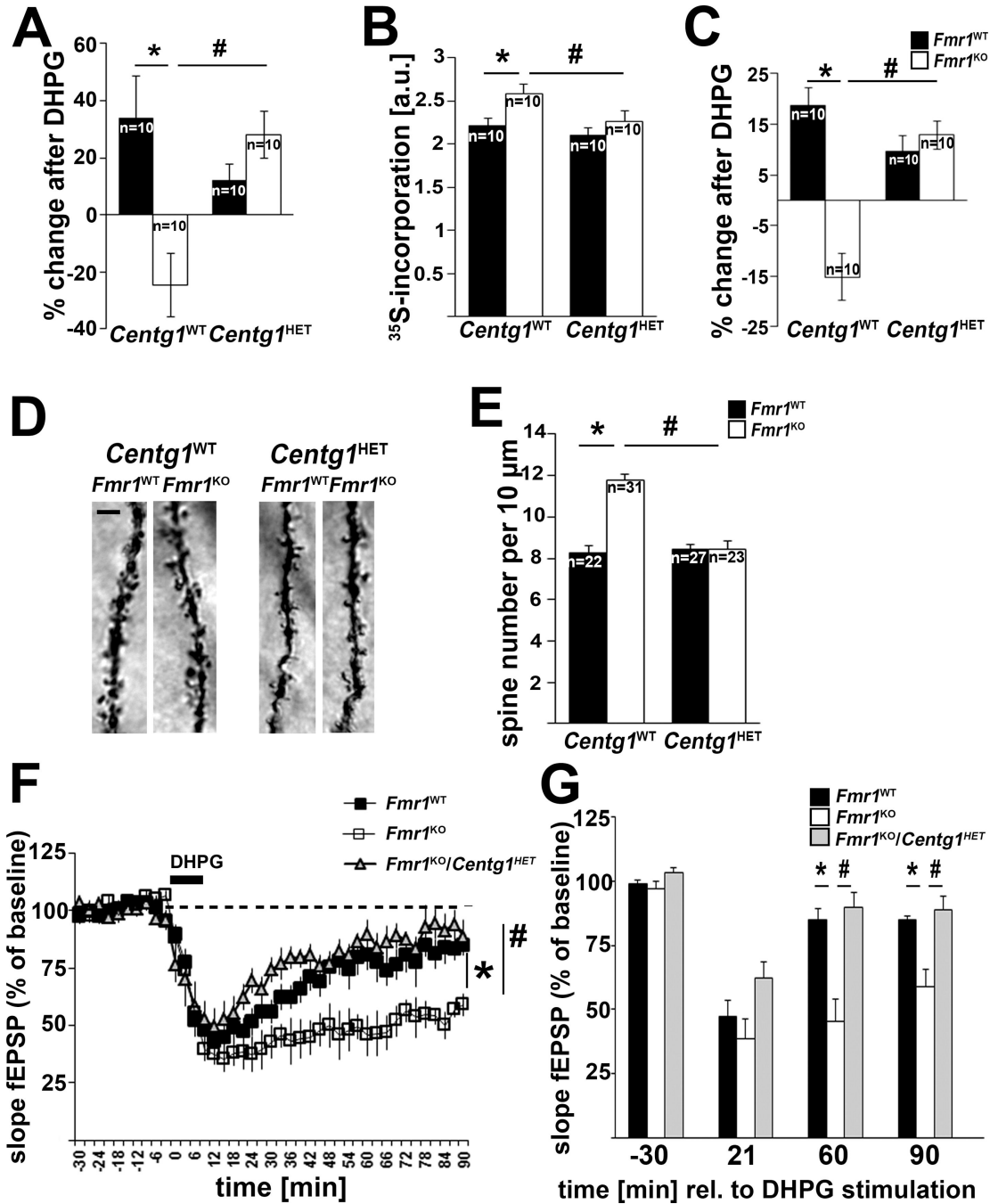


**Figure 2. Genetic reduction of *Centg1* rescues dysregulated mGlu5-mediated PI3K activity and protein synthesis, increased dendritic spine density and impaired synaptic plasticity in *Fmr1*<sup>KO</sup> mice**

(A) Genetic reduction of *Centg1* restores the mGlu1/5-induced increase in p110 $\beta$  enzymatic activity in cortical synaptic fractions (100  $\mu$ M DHPG for 10 min; 2-way ANOVA,  $p(Fmr1)=0.052$ ,  $F(1, 36)=4.0$ ;  $p(Centg1)=0.15$ ,  $F(1,36)=2.2$ ;  $p(interaction)=0.001$ ,  $F(1,36)=12.4$ ; \* $p=0.002$ , # $p=0.006$ ).

(B) Increased basal protein synthesis rates in *Fmr1*<sup>KO</sup> cortical synaptic fractions, as measured by incorporation of radiolabeled amino acids, were significantly reduced to wild

type levels by genetic reduction of *Centg1* (2-way ANOVA,  $p(Fmr1)=0.28$ ,  $F(1, 36)=1.2$ ;  $p(Centg1)=0.043$ ,  $F(1,36)=4.4$ ;  $p(interaction)=0.011$ ,  $F(1,36)=7.1$ ; \* $p=0.053$ , # $p=0.009$ ).

(C) Genetic reduction of *Centg1* restores the mGlu1/5-induced increase in protein synthesis rates in *Fmr1*<sup>KO</sup> cortical synaptic fractions (50  $\mu$ M DHPG for 20 min; 2-way ANOVA,  $p(Fmr1)=0.0001$ ,  $F(1, 36)=18.6$ ;  $p(Centg1)=0.011$ ,  $F(1,36)=7.1$ ;  $p(interaction)<0.0001$ ,  $F(1,36)=27.1$ ; \* $p<0.0001$ , # $p<0.0001$ ).

Error bars represent SEM, n represents individual mice from at least 5 different litters.

(D,E) Genetic reduction of *Centg1* normalizes dendritic spine density in CA1 apical dendrites to wild type levels (2-way ANOVA,  $p(Fmr1)<0.0001$ ,  $F(1, 99)=32.4$ ;  $p(Centg1)<0.0001$ ,  $F(1,99)=27.0$ ;  $p(interaction)<0.0001$ ,  $F(1,99)=33.1$ ; \* $p<0.0001$ , # $p<0.0001$ ). Example images are shown in **D**, quantification of number of dendritic spines per 10  $\mu$ m is shown in **E**. N indicates number of secondary dendrites analyzed (60–100  $\mu$ m length each, starting from the primary shaft), 3–5 mice/genotype, 4–8 neurons/mouse, 1 dendrite/neuron. See Figure S2 for additional analyses. Scale bar is 3  $\mu$ m.

(F,G) Exaggerated DHPG-induced mGluR-LTD in *Fmr1*<sup>KO</sup> hippocampal slices is rescued by *Centg1* heterozygosity. (F) Shown are mean field excitatory postsynaptic potentials (fEPSPs) normalized to baseline as a function of time (*Fmr1*<sup>WT</sup>: n=7, *Fmr1*<sup>KO</sup>: n=8, *Fmr1*<sup>KO</sup>/*Centg1*<sup>HET</sup>: n=9; repeated measures two-way ANOVA (genotype X time),  $n(genotype)=3$ ,  $n(time\ points)=26$ ,  $p(genotype)=0.0013$ ,  $F(2,21)=9.3$ ;  $p(time)<0.0001$ ,  $F(15,525)=12.99$ ;  $p(interaction)<0.0001$ ,  $F(50,525)=2.3$ ; Tukey's posthoc tests: \* $p=0.019$ , # $p=0.001$ ,  $p^{ns}(Fmr1^{wt}/Centg1^{WT}Fmr1^{KO}/Centg1^{HET})=0.595$ ). (G) Average fEPSPs at different time points before and after DHPG treatment shows significantly lower fEPSPs in *Fmr1*<sup>KO</sup> 60 and 90 min post DHPG compared to both *Fmr1*<sup>WT</sup> and *Fmr1*<sup>KO</sup>/*Centg1*<sup>HET</sup>, whereas *Fmr1*<sup>WT</sup> and *Fmr1*<sup>KO</sup>/*Centg1*<sup>HET</sup> were not different from each other (1-way ANOVAs; **-30 min**:  $p=0.106$ ,  $F(2,21)=2.5$ ; **21 min**:  $p=0.055$ ,  $F(2,21)=3.3$ ; **60 min**:  $p=0.0002$ ,  $F(2,21)=13.5$ , \* $p=0.0016$ , # $p=0.0003$ ; **90 min**: (n different than previous time points: *Fmr1*<sup>WT</sup>: n=4, *Fmr1*<sup>KO</sup>: n=4, *Fmr1*<sup>KO</sup>/*Centg1*<sup>HET</sup>: n=5)  $p=0.005$ ,  $F(2,10)=9.4$ , \* $p=0.017$ , # $p=0.006$ ).

Error bars represent SEM.

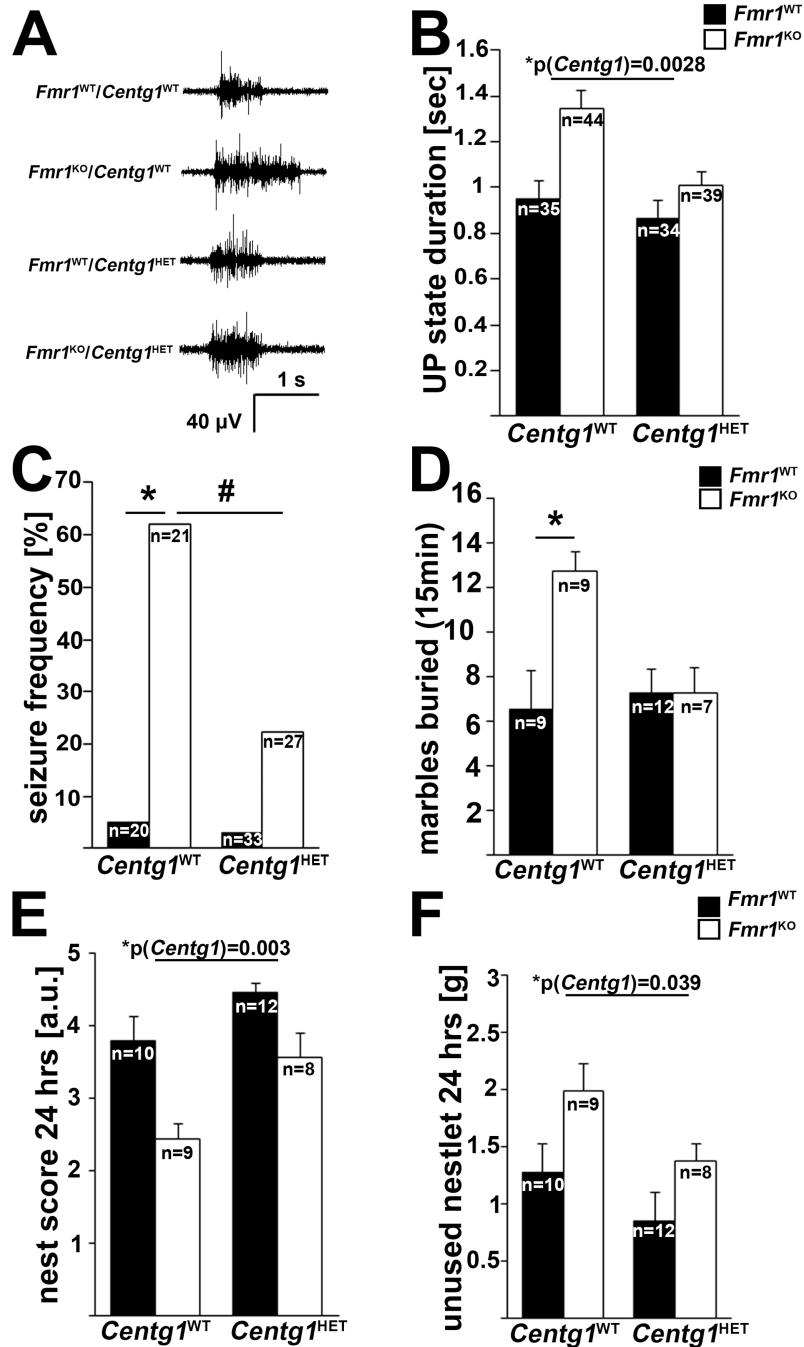


**Figure 3. Genetic reduction of *Centg1* reduces neocortical hyperactivity and repetitive behaviors, and improves nest building in *Fmr1<sup>KO</sup>* mice**

(A,B) Genetic reduction of *Centg1* decreases duration of UP states in acute thalamocortical slices from *Fmr1<sup>KO</sup>* mice. Example traces for each genotype are shown in (A), and quantification in (B) (2-way ANOVA,  $p(\text{Fmr1}) < 0.001$ ,  $F(1, 148) = 15.4$ ;  $p(\text{Centg1}) = 0.002$ ,  $F(1, 148) = 9.8$ ;  $p(\text{interaction}) = 0.131$ ,  $F(1, 148) = 2.3$ , data square root transformed twice to achieve normal distribution). Also see Figures S3A and B showing that UP states in *Fmr1<sup>WT</sup>* and *Fmr1<sup>KO</sup>* thalamocortical slices are independent of PI3K signaling.

(C) Genetic reduction of *Centg1* reduces increased susceptibility to audiogenic seizures in *Fmr1*<sup>KO</sup> mice (Fisher's exact tests, \* $p=0.0002$ ; # $p=0.008$ ;  $p(Fmr1^{WT}/Centg1^{WT}Fmr1^{KO}/Centg1^{HET})=0.213$ ).

(D) Genetic reduction of *Centg1* rescues increased marble burying in *Fmr1*<sup>KO</sup> mice. Shown are number of marbles buried more than 50% after 15 min (2-way ANOVA,  $p(Fmr1)=0.037$ ,  $F(1, 33)=4.7$ ;  $p(Centg1)=0.106$ ,  $F(1,33)=2.8$ ;  $p(interaction)=0.039$ ,  $F(1,33)=4.6$ ; \* $p=0.021$ ). (E,F) Impaired nesting behavior is improved in *Fmr1*<sup>WT</sup> and *Fmr1*<sup>KO</sup> mice by genetic reduction of *Centg1*. Shown are the nest score (E) and the average amount of unused nestlet after 24 hours (F) (E, 2-way ANOVA,  $p(Fmr1)=0.003$ ,  $F(1, 35)=16.1$ ;  $p(Centg1)=0.003$ ,  $F(1,35)=10.0$ ;  $p(interaction)=0.418$ ,  $F(1,35)=0.7$ ; F, 2-way ANOVA,  $p(Fmr1)=0.015$ ,  $F(1, 35)=6.6$ ;  $p(Centg1)=0.039$ ,  $F(1,35)=4.6$ ;  $p(interaction)=0.699$ ,  $F(1,35)=0.15$ ). Representative pictures of nests and analyses after 72 hours are shown in Figures S3C–E.

Error bars represent SEM. N indicates number of slices for B, and individual mice from at least 5 different litters for C–F.

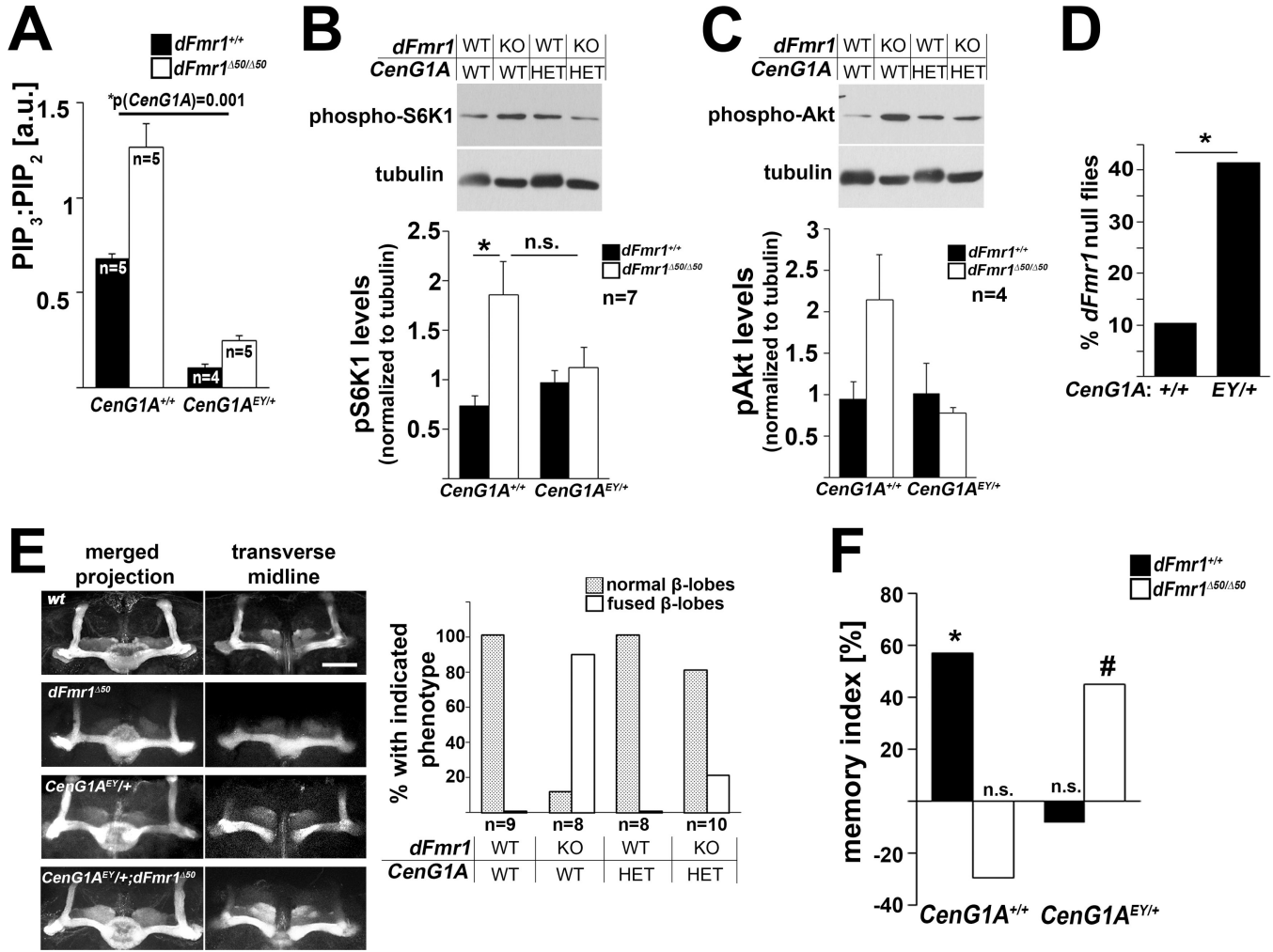


**Figure 4. Genetic reduction of *CenG1A* rescues excessive PI3K activity and neuronal defects in a *Drosophila* model of FXS**

(A) Significantly increased PIP<sub>3</sub>/PIP<sub>2</sub> ratio in *dFmr1*<sup>Δ50</sup> mutant fly heads is decreased by *CenG1A*<sup>EY01217</sup> heterozygosity (2-way ANOVA,  $p(dFmr1)=0.025$ ,  $F(1, 15)=6.2$ ;  $p(CenG1A)=0.001$ ,  $F(1,15)=16.7$ ;  $p(interaction)=0.372$ ;  $F(1,15)=0.8$ ). Also see Figure S4A for confirmation of loss of dFMR1 expression in the *dFmr1* mutant flies.

(B,C) Western blot analyses suggest that increased S6K1 phosphorylation (B) and increased Akt phosphorylation (C) in *dFmr1*<sup>Δ50</sup> mutant fly heads is reduced by genetic reduction of *CenG1A* (B, related samples Friedman's test by ranks,  $p=0.034$ ; Wilcoxon signed rank posthoc analyses:  $*p=0.008$ ,  $p(n.s.)=0.257$ ; C, 2-way ANOVA  $p(dFmr1)=0.194$ ,  $F(1, 12)=1.9$ ;  $p(CenG1A)=0.088$ ,  $F(1,12)=3.5$ ;  $p(interaction)=0.061$ ,  $F(1,12)=4.3$ ).

(D) Viability of *dFmr1*<sup>Δ50</sup> mutant flies is increased (to or above Mendelian ratios) by *CenG1A*<sup>EY01217</sup> heterozygosity ( $n(dFmr1\ \Delta50)=339$ ;  $n(CenG1A^{EY01217};dFmr1\ \Delta50)=331$ , Fisher's exact test  $p<0.001$ ).

(E) Heterozygosity for the *CenG1A*<sup>EY01217</sup> allele rescues  $\beta$ -lobe fusion in mushroom bodies of *dFmr1*<sup>Δ50</sup> mutant flies. Example images of Fasciclin II-stained mushroom bodies are shown as merged z-stack projections (left) and single optical sections through the transverse

midline (right) (Fisher's exact tests:  $p(\text{wt-}dFmr1^{50}) < 0.001$ ,  $p(\text{wt-}CenG1A^{EY}) = 1$ ,  $p(dFmr1^{50}; CenG1A^{EY}; dFmr1^{50}) = 0.006$ ,  $p(\text{wt-}CenG1A^{EY}; dFmr1^{50}) = 0.477$ ). Scale bar is 50  $\mu\text{m}$ .

(F) Heterozygosity for the *CenG1A<sup>EY01217</sup>* allele rescues loss of courtship short-term memory in *dFmr1* mutant flies and impairs courtship memory in wild type background (one-way ANOVA with Sidak's multiple comparison;  $p < 0.0001$ ,  $F(7,227) = 16.5$ ,  $*p = 0.0097$ ,  $\#p = 0.0012$ . <sup>ns</sup> $p > 0.9$ ; n(naïve, trained): wt(48,23); *dFmr1<sup>50</sup>*(30,17); *CenG1A<sup>EY</sup>*(33,24); *CenG1A<sup>EY</sup>; dFmr1<sup>50</sup>*(36,24)). Data are presented as memory index, i.e. the relative difference between the mean courtship index (CI) of trained and naïve flies ((CI(naïve)-CI(trained))/CI(naïve)), average CI $\pm$  SEM are shown in Figure S4B.

Error bars are SEM, n indicated in the figure. N represents individual experiments pooling 15–30 fly heads per condition in A–C, and individual flies in D–F.

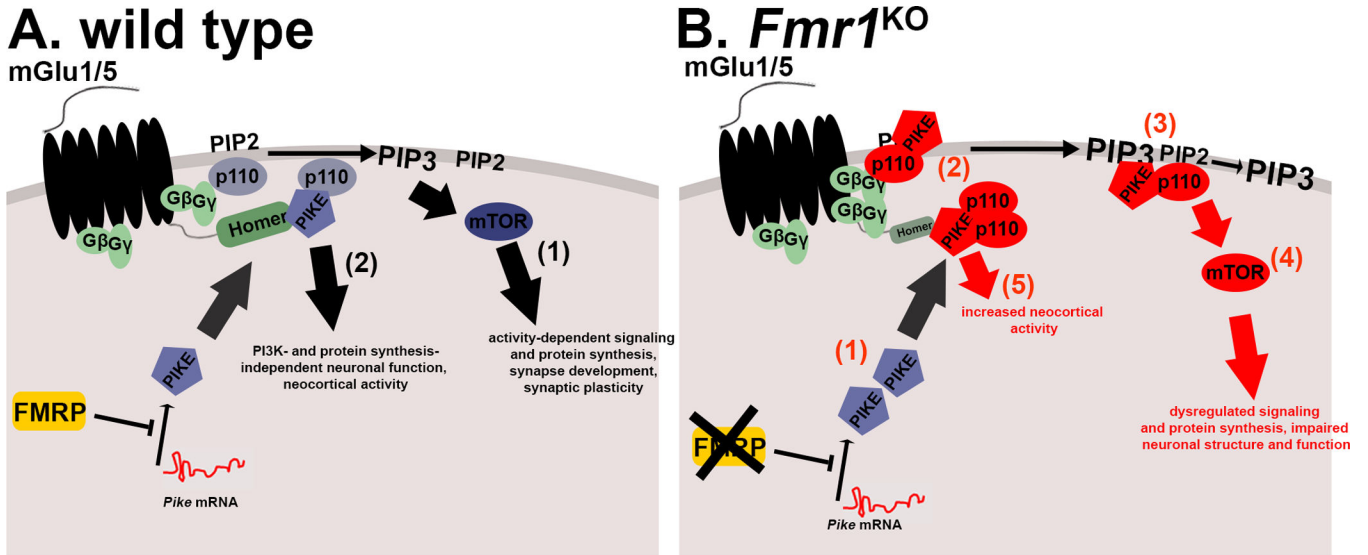


**Figure 5. Proposed simplified model of PIKE's role in dysregulated mGlu5-dependent neuronal functions in FXS**

(A) mGlu5 receptors mediate activation of PI3K catalytic subunits (p110) through either Homer-PIKE scaffolds or through heterotrimeric G proteins ( $G_{\beta\gamma}$ ). FMRP directly regulates expression levels of PIKE, and thus provides crucial control of mGlu5-dependent functions, including PI3K/mTOR-dependent downstream signaling and activity-regulated protein synthesis (1), as well as PI3K- and protein synthesis-independent functions (2).

(B) In the absence of FMRP-mediated translational repression, PIKE levels are elevated (1). This contributes to increased mGlu5-mediated activation of PI3K catalytic subunits (2). Increased PIKE levels may also cause receptor-independent, PIKE-mediated PI3K activation (3), which could contribute to the overall increase in PIP3/PIP2 ratios. Together, this contributes to increased mGlu1/5-mediated PI3K/mTOR signaling, causing defects in protein synthesis and synaptic plasticity (4). In addition, increased PIKE contributes to impairments in other mGlu5-dependent, but protein synthesis- and PI3K-independent neuronal functions, such as prolonged neocortical UP states (5). Our study suggests that reduction of PIKE in *Fmr1*<sup>KO</sup> animal models limits excessive mGlu1/5-dependent downstream signaling, both PI3K dependent and -independent, leading to normalized signal transduction, protein synthesis, neuronal structure and function.